Picosecond circular dichroism spectroscopy: a Jones matrix analysis

Xiaoliang Xie and John D. Simon

Department of Chemistry B-041, University of California, San Diego, La Jolla, California 92093

Received July 20, 1989; accepted November 8, 1989

Measurement of time-resolved circular dichroism signals can be complicated by transient linear dichroism and birefringence effects. These signals arise from using a polarized light beam for excitation and from imperfect modulation of the circularly polarized probe beam. In a polarization-modulation experiment designed to measure the time dependence of circular dichroism, a small amount of pump-induced linear dichroism coupled with birefringence of optics would dominate the observed signals, rendering an accurate measurement virtually impossible. We examine these effects within the Jones matrix formalism. These calculations demonstrate how one can experimentally eliminate transient linear polarization signals, permitting accurate measurement of the transient circular dichoism of a sample with picosecond resolution. Theory and experiment are compared for time-dependent data on myoglobin following the photoelimination of CO from carbonmonoxy myoglobin.

1. INTRODUCTION

Polarization spectroscopy has become an important tool for the study of molecular structure and dynamics.[1-5] In simple cases, one can directly evaluate the linear dichroism, linear birefringence, circular dichroism, and circular birefringence of a sample by performing polarization-modulation experiments. However, for more complicated molecular systems (i.e., crystals and transient spectroscopy), measurements at the modulation frequency can be a complicated function of all these various optical properties. With the development of high-repetition-rate picosecond laser systems, various steady-state polarization techniques have been extended into the time domain, enabling one to measure time-dependent properties of molcules.[6-16]

In this paper we will be concerned with time-resolved circular dichroism (CD) spectroscopy. Our efforts at developing techniques for the collection of time-resolved CD data have been motivated by the fact that CD signals reflect molecular conformation.[17] Development of time-resolved CD spectroscopy could enable one to study time-dependent conformational changes in proteins. In particular, in this paper we focus on time-dependent changes in the CD spectrum of myoglobin following the photodissociation of CO from carbonmonoxy myoglobin. Several of the optical absorption bands of heme proteins [Soret band ($\lambda \approx 400$ nm), N band ($\lambda \approx 350$ nm), and Q band ($\lambda \approx 600$ nm)] exhibit large changes in the CD spectrum, depending on whether a ligand is coordinated to the heme ring[18-23]; for example, the CD of the N band at 355 nm changes from a negative value in carbonmonoxy myoglobin to zero in myoglobin. These transitions provide information on the protein conformation in the vicinity of the heme ring, and a time-dependent CD study of these optical transitions could be used to examine the conformation relaxation that occurs in myoglobin following ligand photodissociation.

As a result of the potential importance of transient CD spectroscopy as a tool for studying protein conformational changes, several different approaches have been pursued in recent years.[24-29] Microsecond or millisecond resolution was achieved by using polarization modulation coupled to a stop-flow[24] or flash photolysis[25] apparatus, respectively. The ultimate time resolution of a simple flash photolysis apparatus was limited by the modulation rate of the piezoelectric devices used to generate the probe light beams, which is of the order of 50 kHz, giving rise to slightly better than millisecond time resolution. Stop-flow techniques were found to extend the time resolution into the microsecond regime. Recently Kliger and co-workers[26-29] achieved nanosecond resolution by using an elegant variation on the optical arrangement used to measure steady-state ellipticity. Using this technique, they examined protein relaxation in myoglobin, finding that the transient CD spectrum changes from that characteristic of carbonmonoxy myoglobin to that of myoglobin within the resolution of the instrument. Measurements of the order of the instrument response were also complicated by large transient signals. Comparison with theory demonstrated that these signals arose from pump-induced linear birefringence effects in the sample. The results from their studies indicated that higher time resolution was required for observation of the conformational change in myoglobin following ligand loss.

Recently we reported a technique for the determination of transient CD measurements whose temporal resolution is limited by the laser pulse width.[30] This approach extended time-resolved CD spectroscopy into the picosecond domain, enabling one to study fast conformational motions in proteins. The experimental technique is an extension of the polarization-modulation technique used in commercial CD spectrometers. However, in our early attempt to extend this approach into the time domain, we found that the observed signal would vary significantly with experimental conditions. In particular, using depolarized, circularly polarized, or linearly polarized excitation light produced different transient signals. Furthermore, the magnitude and the time dependence of the transient

0740-3224/90/081673-12$02.00

signals were dependent on the purity of the circularly polarized probe beam; different degrees of ellipticity produced different signals. These results suggested that the signal observed was sensitive to other polarization properties of the sample in addition to CD.

Similar effects were encountered in experimental measurements of rotational diffusion made using an anisotropic absorption technique.[7] This technique, developed by Shank and Ippen,[12] involved the measuring of the linear dichroism of a sample, using linear polarized pump and probe pulses that are rotated 45° from each other. The intensity of the probe pulse is then analyzed through a crossed polarizer. Observation of light intensity through the analyzed polarizer signifies that the sample has rotated the polarization vector of the light, rendering a measurement of the linear dichroism of the sample. However, Waldeck *et al.*[7] demonstrated that the interaction between the polarization of the photoexcitation pulse and the birefringence of the optical components in the experimental apparatus could significantly distort the observed signals. For an accurate determination of rotational diffusion times, the contribution of these pump-induced polarization effects needed to be addressed. Another method of measuring rotational diffusion was developed by von Jena and Lessing.[10,11] In this approach, a Pockels cell periodically switches the probe beam between two orthogonal polarizations, and phase-sensitive detection is used to measure the signal. The advantage of this technique is that it is free from the influence of linear birefringence, as the vertical and horizontal polarized light is passed through the sample separately.

Unfortunately, CD signals are generally 1 or 2 orders of magnitude weaker than those observed in linear dichroism experiments. Thus complications from pump-induced linear dichroism and linear birefringence, coupled with the external birefringence of the experimental apparatus, could render a measurement of transient CD signal difficult, if not impossible. In this paper we examine how the external birefringence and the pump-induced linear birefringence and dichroism affect the measurement of time-resolved CD data. Using Jones matrix calculus,[31–37] we can show how these effects can be eliminated, allowing one to measure time-dependent CD accurately for any sample of interest. Theory and experiment are compared for studies on the transient CD signal for the N band of myoglobin following photodissociation of CO from carbonmonoxy myoglobin. These results are the first picosecond time-resolved CD data on a protein to our knowledge and provide information on the conformation relaxation following ligand photodissociation.

In writing this paper we have tried to describe the physical origins of various polarization effects, in addition to providing rigorous mathematical treatments. The ideas and results are not only relevant to picosecond time-resolved CD but are also instructive for steady-state CD measurement of oriented molecules or crystalline samples.

The remainder of this paper is organized as follows. The experimental apparatus for collecting time-resolved CD data is described in Section 2. In Section 3 the Jones matrix calculus is used to examine the contributions of various polarization effects to the observed experimental signal. In Section 4 experimental results on the time-resolved CD changes in myoglobin following photodissociation of CO from carbonmonoxy myoglobin under various experimental conditions are examined and compared with the theoretical calculations. This is followed by concluding remarks in Section 5.

2. EXPERIMENT

A complete description of the experimental apparatus was recently reported.[30,38] A continuous-wave, mode-locked, Q-switched, and cavity-dumped ND:YAG laser and a tunable cavity-dumped dye laser are used to generate picosecond pulses at a 1.0-kHz repetition rate. These pulses are used for excitation and for probing the sample. In Fig. 1 we show the optical arrangement used to measure the transient CD. The probe beam is passed through an electro-optic modulator, which generates a train of alternating left and right circularly polarized laser pulses. The resulting modulation frequency is 500 Hz. This modulated probe beam is focused into a spinning sample cell with a 2-mm path length. The spinning rate of the cell is sufficient that each pump pulse excites a fresh sample, avoiding the effects of both thermal lensing in the sample and the photolysis of photoproducts. The transmitted probe light is detected by a rf-shielded photomultiplier (RCA 1P28 in a Pacific Instruments housing). The signal is amplified by a broadband preamplifier (LeCroy Model VV100BTB) and then fed into a sample-and-hold circuit (SRS Model 250), effectively increasing the duty cycle. The output from the sample-and-hold circuit is nearly a square wave and thus is similar to the signal detected in conventional CD spectrometers. This output is sent to a lock-in amplifier (EGG Model 5209), which is referenced to the polarization-modulation frequency. With a 3–10-sec time constant, we obtain a signal-to-noise ratio of >10:1. Both the output from the lock-in amplifier and the sample-and-hold circuits are digitized by 16-bit analog-to-digital converters and processes by an IBM PC-AT computer.

After traversing a computer-controlled optical delay line, the pump beam passes through a depolarizer and a spinning half-wave plate combination before being focused into the sample. As will be shown below, these optics remove all contributions of pump-induced linear birefringence and dichroism to the detected signal. Without these optics, the time-dependent signal depends strongly on the optical alignment (Section 4 below). Varying the time delay between each pump–probe pulse pair enables

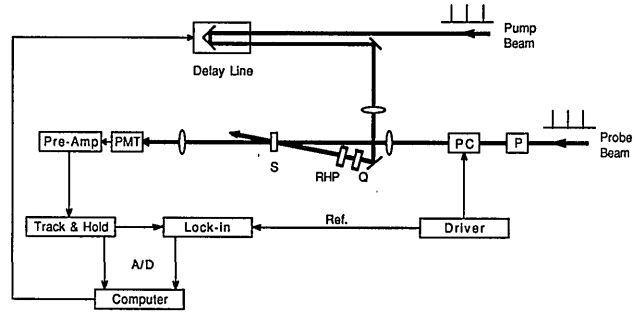

Fig. 1. Schematic of the optical arrangement used to measure time-resolved CD data: PC, Pockels cell; Q_4, quarter-wave plate or depolarizer; RHP, rotating half-wave plate; S, sample cell; P, polarizer; PMT, photomultiplier tube, A/D, analog-to-digital converter.

the evolution of the CD signal at a fixed wavelength to be determined. On the other hand, scanning the probe dye laser at a fixed time delay between the pump and probe pulses can generate a transient CD spectrum.

3. THEORY

A. Jones Matrix Calculus

Jones matrix calculus[31–37] provides a convenient framework for analyzing the effects of optical components on light beams with well-defined polarizations. Assuming that the light is propagating in the z direction, the polarization vector of the light in the x,y plane can be described by a column matrix:

$$J = \begin{bmatrix} E_x \\ E_y \end{bmatrix} = \begin{bmatrix} E_{x0} \exp[i(\omega t + \phi_x)] \\ E_{y0} \exp[i(\omega t + \phi_y)] \end{bmatrix}, \tag{1}$$

where E_{x0} and E_{y0} are the amplitudes of the x and y components and ϕ_x and ϕ_y are the corresponding phase shifts. The intensity of the light beam is given by $E^2 = \bar{E}_x E_x + \bar{E}_y E_y$. In this paper we will be concerned with the propagation of circularly polarized light through the experimental apparatus. Left and right circularly polarized light can be represented by $E_{x0} = E_{y0} = E_0$, $\phi_x = \pi/2$, $\phi_y = 0$ and $E_{x0} = E_{y0} = E_0$, $\phi_x = -\pi/2$, $\phi_y = 0$, respectively. We can ignore the time-dependent term, ωt, as both circularly polarized beams have the same time dependence. Thus the corresponding column matrices for the left and right circularly polarized light are

$$J_L = \begin{bmatrix} E_0 \exp\left(i\frac{\pi}{2}\right) \\ E_0 \end{bmatrix}, \qquad J_R = \begin{bmatrix} E_0 \exp\left(-i\frac{\pi}{2}\right) \\ E_0 \end{bmatrix}, \tag{2}$$

respectively.

The effect of an optical element on the probe light can be described by multiplying the appropriate M matrix (a 2 by 2 matrix that describes the polarization properties of the optical element) by the above column matrices. The resulting product is a new column matrix that represents the output light. For example, if left and right circularly polarized light beams are independently passed through a linearly birefringent optic followed by a CD sample, one would evaluate the products

$$\begin{bmatrix} \text{circular} \\ \text{dichroism} \end{bmatrix} \times \begin{bmatrix} \text{linear} \\ \text{birefringence} \end{bmatrix} \times J_L \tag{3}$$

and

$$\begin{bmatrix} \text{circular} \\ \text{dichroism} \end{bmatrix} \times \begin{bmatrix} \text{linear} \\ \text{birefringence} \end{bmatrix} \times J_R. \tag{4}$$

From these two expressions, one could calculate the effect of these polarization properties on the transmitted (or detected) circularly polarized probe light beams, E_L^2 and E_R^2.

However, in many cases, an optic (or sample) can exhibit many polarization properties. As an example, a sample can be both linearly birefringent and circularly dichroic. A complication arises, as the Jones matrices for linear birefringence and CD do not commute. Thus the matrix that describes the sample depends on the order of matrix multiplication. This would lead to two different formulas for E_L^2 and E_R^2, neither of which would accurately describe the transmitted light beam.

In order to treat the case in which an optical element exhibits several different properties whose M matrices do not commute, one can divide the element into small slices and evaluate the polarization of the transmitted light after each consecutive slice, using Jones calculus. Each slice is further viewed as composed of subslices that individually exhibit the various optical properties characteristic of the total element. If the number of the slices is large (i.e., infinitesimally thin slices), the final result should be independent of the order of subslices. The method was quantified by Jones in 1942[34] and is commonly referred to as the N-matrix technique.

The N matrix is defined as

$$N = (\mathrm{d}M/\mathrm{d}z)M^{-1}, \tag{5}$$

where z is the distance through the optic being modeled. Using this equation, one can construct the N matrix of any optical property from the corresponding M matrix. The N matrices for linear birefringence, linear dichroism, circular birefringence, and CD have been tabulated.[34,39]

For an optical element that exhibits several different properties, the total N matrix is the sum of the N matrices corresponding to the various individual optical properties. According to Eq. (5), under the condition that the optical element is homogeneous along the z direction, i.e., N independent of z, the M matrix can be obtained by

$$M = e^{Nz}. \tag{6}$$

The details of this procedure can be found in a number of sources (e.g., Refs. 34 and 39). The resulting expressions are given in Eqs. (7)–(14) below. These expressions will be used to carry out N-matrix calculations in the balance of this paper.

Given the N matrix

$$N = \begin{bmatrix} n_1 & n_4 \\ n_3 & n_2 \end{bmatrix}, \tag{7}$$

the corresponding M matrix is

$$M = \exp^{Tz} \times \begin{bmatrix} m_1 & m_4 \\ m_3 & m_2 \end{bmatrix}, \tag{8}$$

where

$$T = (n_1 + n_2)/2, \tag{9}$$

$$Q = [\tfrac{1}{4}(n_1 - n_2)^2 + n_3 n_4]^{1/2}, \tag{10}$$

and the matrix elements of M are

$$m_1 = \cosh(Qz) + \frac{1}{2Q}(n_1 - n_2)\sinh(Qz), \tag{11}$$

$$m_2 = \cosh(Qz) - \frac{1}{2Q}(n_1 - n_2)\sinh(Qz), \tag{12}$$

$$m_3 = \frac{1}{Q} n_3 \sinh(Qz), \tag{13}$$

$$m_4 = \frac{1}{Q} n_4 \sinh(Qz), \tag{14}$$

B. Polarization Modulation and Circular Dichroism

In this subsection we consider the measurement of the CD of a sample with no complications from other polarization effects. In particular, we consider the case in which pure left and right circularly polarized light are alternately passed through a circularly dichroic sample. It should be pointed out that most conventional CD spectrometers use sinusoidal modulation; however, we have chosen to examine a square-wave modulation, as this resembles what is used in carrying out our time-dependent studies. In this case, the resulting differential absorption can be related to the transmitted intensities as follows:

$$\Delta A = (\Delta\varepsilon)cl = \log(I_R/I_0) - \log(I_L/I_0) = \log(I_R) - \log(I_L)$$
$$= \Delta\log(I) \approx \frac{\Delta I}{2.303 \times I}. \tag{15}$$

In the above expression, c is the sample concentration, l is the cell path length, and I_0 is the intensity of left and right circularly polarized light before it enters the sample. I_R and I_L are the corresponding intensities after the light has passed through the sample; their difference and mean are signified by ΔI and I, respectively. To carry out such a measurement in practice, one needs to determine the ratio of the ac and dc components of the modulated signal. In the notation introduced in Subsection 2.A, this signal is proportional to

$$\frac{E_L^2 - E_R^2}{E_L^2 + E_R^2}. \tag{16}$$

In the perfect case of no complications from any polarization artifacts, expression (16) can be evaluated within the Jones matrix calculus. The M matrix for circular dichroism is given by

$$M_{CD} = \frac{1}{2}\begin{bmatrix} k + k' & -i(k - k') \\ i(k - k') & k + k' \end{bmatrix}, \tag{17}$$

where k'^2 and k^2 are the transmittance of left and right circularly polarized light, respectively. Performing the multiplication of M_{CD} by J_L and J_R, followed by the evaluation of E_R^2 and E_L^2, gives the following result:

$$\frac{E_L^2 - E_R^2}{E_L^2 + E_R^2} = \frac{k'^2 - k^2}{k'^2 + k^2}. \tag{18}$$

As expected, this is proportional to the circular dichroism of the sample.

C. Effect of Sample Circular Birefringence

One of the major advantages of the polarization-modulation technique is that the measurement is free from the influence of the circular birefringence of the sample. Circular birefringence (CB) is characterized by an optical rotation in which the polarization of a linearly polarized light beam is rotated by a chiral sample. In order to show that the detected signal is free from CB, the Jones calculus can be used. The Jones matrix for CB is expressed by

$$M_{CB} = \begin{bmatrix} \cos(\delta z) & -\sin(\delta z) \\ \sin(\delta z) & \cos(\delta z) \end{bmatrix}, \tag{19}$$

where $\delta = \pi(n_R - n_L)/\lambda$. In this expression, λ is the wavelength of the incident light, n_R and n_L are the index of refraction of the sample with respect to right and left circularly polarized light, respectively, and z is the path length of the sample.

The matrices for CD and CB commute. Multiplication of the product of M_{CD} and M_{CB} by the column vectors J_L and J_R, followed by the evaluation of E_L^2 and E_R^2, gives Eq. (18). This result demonstrates that the CB of the sample does not effect the experimental measurement of CD.

At this point, it is instructive to carry out the above calculation, using the N-matrix technique. This case will serve to show the equivalence of the N-matrix calculus and the M-matrix methods. Using Eq. (5), the N matrices for CB, N_{CB}, the CD, N_{CD}, can be evaluated. The resulting expressions are

$$N_{CB} = \delta\begin{bmatrix} 0 & -1 \\ 1 & 0 \end{bmatrix}, \tag{20}$$

$$N_{CD} = -0.575c\begin{bmatrix} \varepsilon_L + \varepsilon_R & i(\varepsilon_L - \varepsilon_R) \\ -i(\varepsilon_L - \varepsilon_R) & \varepsilon_L + \varepsilon_R \end{bmatrix}. \tag{21}$$

In the expression for N_{CD}, ε_R and ε_L are the extinction coefficients of the sample with respect to right and left circularly polarized light, respectively. The total N matrix is given by the sum of Eqs. (20) and (21). Using Eqs. (7)–(14), the elements of the M matrix can be determined. Letting $\gamma = 0.575c(\varepsilon_L - \varepsilon_R)$, one obtains

$$Q = \gamma - i\delta, \tag{22}$$

$$T = -0.575(\varepsilon_L + \varepsilon_R), \tag{23}$$

and

$$M_{CD,CB} = e^{T_z}\begin{bmatrix} \cosh[(\gamma - i\delta)z] & -i\sinh[(\gamma - i\delta)z] \\ i\sinh[(\gamma - i\delta)z] & \cosh[(\gamma - i\delta)z] \end{bmatrix}. \tag{24}$$

Since each term in the resulting signal expression, Eq. (18), will contain e^{2T_z}, this factor need not be considered in the calculation. Straightforward multiplication of $M_{CD,CB}$ by J_L and J_R results in the expressions for the transmitted intensities, E_L^2 and E_R^2, respectively. The resulting signal is

$$\frac{E_L^2 - E_R^2}{E_L^2 + E_R^2} = \frac{e^{-2\gamma z} - e^{2\gamma z}}{e^{-2\gamma z} + e^{2\gamma z}} = \frac{k'^2 - k^2}{k^2 + k'^2}. \tag{25}$$

Thus, as expected, the circular birefringence of the sample does not affect the measurement of CD.

We now turn to analyze experimental complications that might induce measurement artifacts.

D. Effect of the External Birefringence

A common complication in carrying out CD measurements arises from the fact that optical components between the modulator and the sample (e.g., the sample cell, lenses, and Pockels cell windows) possess strain birefringence. The total linear birefringence (LB) of these optical components can be modeled as a retardation plate, which can be expressed by the following matrix representation, M_{LB}:

$$M_{LB} = \begin{bmatrix} \cos^2\theta e^{ib} + \sin^2\theta e^{-ib} & i\sin 2\theta \sin b \\ i\sin 2\theta \sin b & \cos^2\theta e^{-ib} + \sin^2\theta e^{ib} \end{bmatrix}. \tag{26}$$

In the above matrix, θ is the angle of the fast axis of the optic with respect to the x axis and $2b$ is the retardation.

This matrix commutes with the matrix representation of the CD of the sample. Thus evaluation of $M_{CD} \times M_{LB} \times J_L$ and $M_{CD} \times M_{LB} \times J_R$ results in the following calculated signal:

$$\frac{E_L^2 - E_R^2}{E_L^2 + E_R^2} = \frac{k'^2 - k^2}{k^2 + k'^2} \cos 2b. \quad (27)$$

The signal measured is reduced from the true value of the CD of the sample $[(k'^2) - k^2)/(k'^2 + k^2)]$ by the LB of the cell and optics ($\cos 2b$). It is important to point out that the reduced signal is independent of the orientation of the fast axis (θ). The effect of LB is to convert a circularly polarized beam into an elliptically polarized beam. In an extreme case where $2b = 90°$, the optics mimic a quarter-wave plate, and the circular probe beams are converted into linearly polarized light beams before passing through the sample. In this case, the detected signal reduces to zero. Fortunately, the LB of the optics is generally of the order of $2b \ll 10°$. In this case, $\cos(2b) > 0.985$, and the reduction in signal resulting from the LB of the optical setup is less than 1%.

We now consider the relative orientations of two polarization ellipses after the left and right circularly polarized light passes through this effective retarder. To simplify the calculation, we choose $\theta = 45°$. In this case, M_{LB} becomes

$$M_{LB}(\theta = 45°) = \begin{bmatrix} \cos b & i \sin b \\ i \sin b & \cos b \end{bmatrix}. \quad (28)$$

Evaluating $M_{CD} \times J_L$ results in the following expression for the light vector:

$$\begin{bmatrix} E_x \\ E_y \end{bmatrix} = \begin{bmatrix} E_0(\cos b + \sin b) \exp\left[i\left(\omega t + \frac{\pi}{2}\right)\right] \\ E_0(\cos b - \sin b) \exp(i\omega t) \end{bmatrix}. \quad (29)$$

Eliminating the variable t results in an expression that relates E_x to E_y:

$$\left[\frac{E_x}{(\cos b + \sin b)E_0}\right]^2 + \left[\frac{E_y}{(\cos b - \sin b)E_0}\right]^2 = 1. \quad (30)$$

Therefore the resulting polarization ellipse has its long and short axes along x and y axes, both of which are at a 45° angle with respect to the fast and slow axes of the birefringence. The ratio of the short and long axes of the ellipse is given by $(\cos b - \sin b)/(\cos b + \sin b)$.

Similarly, evaluating $M_{LB} \times J_R$ gives

$$\left[\frac{E_x}{(\cos b - \sin b)E_0}\right]^2 + \left[\frac{E_y}{(\cos b + \sin b)E_0}\right]^2 = 1, \quad (31)$$

with the short and long axes switched from those given in Eq. (30). This indicates that the effect of the LB on the left and right circularly polarized beams is to generate two orthogonal elliptically polarized beams that bisect the fast and slow axes of the birefringence. We will refer back to this fact later in this paper.

Generation of pure circular polarized light with an electro-optic modulator depends on several variables. An imperfectly modulated beam can result from an uncollimated incoming light beam or from misalignment of the beam with respect to the crystal axis. This is because any light beam deviating from the crystal axis of a Pockels cell experiences an inherent birefringence, even when no voltage is applied. We have experimentally examined the output of our Pockels cell and found that the modulator often generates two perpendicular elliptically polarized beams with identical intensity. In light of the above discussion, this observation indicates that the modulator output can be well modeled as circularly polarized light that has been passed through a retardation plate. In the actual case of imperfect modulation, the ratio of short and long axes is generally found to be $\approx 4:5$. Evaluating $(\cos b - \sin b)/(\cos b + \sin b) = 4/5$ gives $\cos 2b \approx 0.98$. Thus the imperfect modulation of the light would reduce the true CD signal by $\approx 2\%$.

Imperfect modulation can also result from using a voltage slightly different from that required for perfect quarter-wave rotation. The effect of imperfect modulation can be modeled by a linearly polarized light beam passing through a retarder with its fast (or slow) axis 45° with respect to the polarization vector [similar to Eq. (28)]. In this case, the resulting light now has a retardation now of $\pm 2\alpha$ rather than $\pm 90°$. Multiplying the Jones matrix of the modulator by a column matrix representing the linear polarized light,

$$\begin{bmatrix} \cos \alpha & \pm i \sin \alpha \\ \pm i \sin \alpha & \cos \alpha \end{bmatrix} \times \begin{bmatrix} 1 \\ 0 \end{bmatrix} = \begin{bmatrix} \cos \alpha \\ \pm i \sin \alpha \end{bmatrix}, \quad (32)$$

gives the imperfectly modulated light. It is straight forward to show that the modulator generates two overlapped (not orthogonal) polarization ellipses with different senses.

Multiplying the M_{CD} by the above column matrices for imperfectly modulated light yields a detected signal of

$$\frac{E_L^2 - E_R^2}{E_L^2 + E_R^2} = \frac{k'^2 - k^2}{k^2 + k'^2} \sin 2\alpha. \quad (33)$$

Thus the signal is reduced from the true value of CD. However, even for $2\alpha = 90° \pm 10°$, corresponding to the maximum effect of maximum nonprecise quarter-wave voltage, $\sin 2\alpha = 0.985$. Thus the reduction in signal is negligible. We will neglect this effect in the following discussion and consider only the case of perfectly modulated light.

E. Effect of the Linear Dichroism and Birefringence of the Sample

An isotropic sample (i.e., a sample in solution) does not possess linear dichroism or birefringence. However, excitation by a polarized beam can break the isotropy. Thus the treatment of polarized excitation on CD measurements is the same as that for evaluating linear dichroism and birefringence properties on CD measurements of nonisotropic uniaxial crystalline samples.[40]

For polarized excitation, as well as uniaxial crystals, there exists only one pair of perpendicular axes for referencing both the linear dichroism (LD) and the LB. These two axes are defined along the x and y axes. In these cases, the resulting Jones matrix for the sample LD is given by

$$M'_{LD} = \begin{bmatrix} m & 0 \\ 0 & m' \end{bmatrix}, \quad (34)$$

where m^2 and m'^2 are the transmissions of the two perpendicular linear polarization axes.

The Jones matrix for the sample LB is

$$M'_{\mathrm{LB}} = \begin{bmatrix} e^{-i\rho} & 0 \\ 0 & e^{i\rho} \end{bmatrix}, \tag{35}$$

where 2ρ is the retardation angle.

The two diagonal matrices given in Eqs. (34) and (35) commute; thus the Jones matrix for LD and LB, $M'_{\mathrm{LB,LD}}$, is simply the product.

Unfortunately, M_{CD} does not commute with $M'_{\mathrm{LB,LD}}$. Physically, this is not surprising, as the effect of LD and LB on the light beam as it passes through the sample is to change the degree of ellipticity, causing a reduction in CD signal, which depends on how far the light has traveled through the sample. A rigorous evaluation is possible by using the Jones N-matrix method outlined in Subsection 2.A. In the remainder of this section we will examine the two limiting cases, (1) $M'_{\mathrm{LB,LD}} \times M_{\mathrm{CD}} \times J_{L,R}$ and (2) $M_{\mathrm{CD}} \times M'_{\mathrm{LB,LD}} \times J_{L,R}$, as well as the expression derived with the N-matrix calculus. Numerical calculations demonstrate that the N-matrix result is intermediate between the two limiting expressions.

For the limiting case in which the effects of LB and LD are evaluated after the CD of the sample is measured, $M'_{\mathrm{LB,LD}} \times M_{\mathrm{CD}} \times J_{L,R}$, the detected signal is given by

$$\frac{E_L^2 - E_R^2}{E_L^2 + E_R^2} = \frac{k'^2 - k^2}{k'^2 + k^2}. \tag{36}$$

This is expected, as there are no polarizers between the sample and the photomultiplier tube; thus any changes in the polarization of the probe beams after they pass through the circularly dichroic sample would not result in an intensity change.

In the other limiting case, the detected signal is given by

$$\frac{E_L^2 - E_R^2}{E_L^2 + E_R^2} = \frac{k'^2 - k^2}{k^2 + k'^2} \frac{2mm'}{m^2 + m'^2} \cos 2\rho. \tag{37}$$

The signal is reduced from the true value of the CD of the sample.

One would expect that the efffect of the LD and LB of the sample is underestimated in case (1) but overestimated in case (2). The real signal should be between that predicted by these two expressions. In order accurately to evaluate the effect of sample birefringence and dichroism on the CD measurement, the product of M_{CD} and $M'_{\mathrm{LB,LD}}$ must be calculated, using the N-matrix formalism.

The N matrices for CD, LB, and LD can be determined as shown in expression (5). The resulting expressions are given in Eqs. (38)–(40) below:

$$N_{\mathrm{CD}} = -0.575c \begin{bmatrix} \varepsilon_R + \varepsilon_L & i(\varepsilon_L - \varepsilon_R) \\ -i(\varepsilon_L - \varepsilon_R) & (\varepsilon_R + \varepsilon_L) \end{bmatrix}, \tag{38}$$

$$N_{\mathrm{LD}} = -1.15c \begin{bmatrix} \varepsilon_x & 0 \\ 0 & \varepsilon_y \end{bmatrix}, \tag{39}$$

$$N_{\mathrm{LB}} = g \begin{bmatrix} i & 0 \\ 0 & -i \end{bmatrix}. \tag{40}$$

In the above matrices, c is the sample concentration, $g = \pi(n_y - n_x)/\lambda = \rho/z$, and ε_x and ε_y are the extinction coefficients of the sample with respect to linearly polarized light propagating along the x and y axes, respectively. In order to simplify the resulting expressions, the following substitutions are made:

$$\gamma = 0.575c(\varepsilon_L - \varepsilon_R), \tag{41}$$

$$\beta = 0.575c(\varepsilon_x - \varepsilon_y). \tag{42}$$

Using Eqs. (9) and (10), one finds that

$$Q = (\beta^2 + \gamma^2 - g^2 - 2ig\beta)^{1/2} \tag{43}$$

and

$$T = -0.575c(\varepsilon_R + \varepsilon_L) - 0.575c(\varepsilon_x + \varepsilon_y). \tag{44}$$

Substitution of these equations into Eqs. (8) and (11)–(14) generates the following M matrix for representing the combined effects of sample LB, LD, and CD, $M_{\mathrm{LB,LD,CD}}$:

$$M_{\mathrm{LB,LD,CD}} = e^{Tz} \begin{bmatrix} \cosh(Qz) - \frac{1}{Q}(\beta - ig)\sinh(Qz) & -\frac{1}{Q}i\gamma \sinh(Qz) \\ \frac{1}{Q}i\gamma \sinh(Qz) & \cosh(Qz) + \frac{1}{Q}(\beta - ig)\sinh(Qz) \end{bmatrix}. \tag{45}$$

Multiplication of the above M matrix by the column vectors, J_L and J_R, permits the evaluation of the transmitted intensities, E_L^2 and E_R^2, respectively. From these expressions, the calculated signal [expression (16)] can be derived. The result is

$$\frac{E_L^2 - E_R^2}{E_L^2 + E_R^2} = \frac{-\gamma[Q \cosh(Qz)\sinh(\bar{Q}z) + \bar{Q}\sinh(Qz)\cosh(\bar{Q}z)]}{Q\bar{Q}\cosh(Qz)\cosh(\bar{Q}z) + (g^2 + \beta^2 + \gamma^2)\sinh(Qz)\sinh(\bar{Q}z)}. \tag{46}$$

In the above expression, $\bar{Q}$ is the complex conjugate of Q. Before comparing it with the two cases described above [Eqs. (36) and (37)], we can evaluate Eq. (46) in various limits. If there were no sample LB or LD, then $\beta = g = 0$, $Q = \bar{Q} = \gamma$, and the above expression would simplify to

$$\frac{E_L^2 - E_R^2}{E_L^2 + E_R^2} = \frac{-2\sinh(\gamma z)\cosh(\gamma z)}{\sinh^2(\gamma z) + \cosh^2(\gamma z)} = \frac{k'^2 - k^2}{k^2 + k'^2}. \tag{47}$$

Thus one recovers the CD of the sample when there is no LB or LD.

In order to examine intermediate cases, one can carry out numerical calculations comparing the N-matrix result, Eq. (46), with the two limiting expressions given by Eqs. (36) and (37). In Fig. 2 we present a calculation of the effect of sample LD on the magnitude of the observed signal. For simplicity, the LB was set equal to

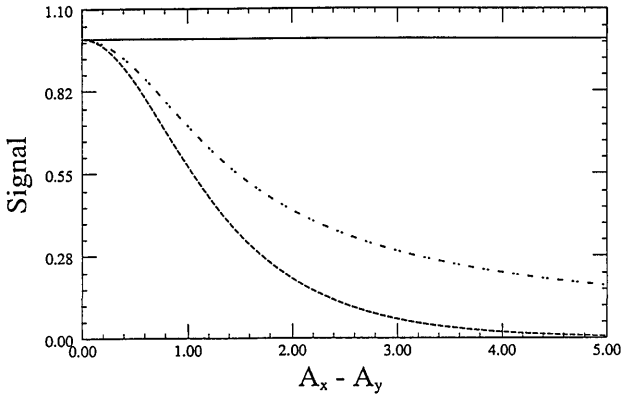

Fig. 2. The effect of linear dichroism on the CD signal is evaluated. The limiting expressions, Eq. (36) (solid line) and (37) (dashed curve), are compared with the N-matrix result, Eq. (46) (dotted–dashed curve). In calculating these curve, $A_L = 5.0$, $A_L - A_R = 0.001, A_x = 5.0$, and $g = 0$. All curves are normalized to 1. The plotted curves show that the LD of the sample reduces the observed signal. The N-matrix calculation results in a curve that is intermediate between the two limiting cases.

zero [$g = 0$ in Eq. (46), $\rho = 0$ in Eq. (37)]. In this calculation, $A_L = 5$ and $A_L - A_R = 0.001$. These values were chosen as they approximate the experimental conditions. The solid line is a plot of Eq. (36). This signal is the true CD signal of the sample. When the limiting equation, Eq. (37), is used, the effect of LD is to reduce the observed signal, as shown by the dashed curve. A 20% difference between the absorption of parallel and perpendicular light results in a reduction of the experimental signal by ≈50%. The dotted–dashed curve is the result of the N-matrix calculation, Eq. (46). As expected, the LD of the sample results in a decreased signal, but smaller than that predicted by the limiting-case expression given by Eq. (37). Calculations that also include LB (g, $\rho \neq 0$) result in a further reduction of signal for a given value of LD. Thus, together, these effects can significantly reduce the observed signal from the value of the CD of the sample.

F. Combined Interaction of External Birefringence and Linear Polarization Effect of the Sample

If one separately considers the effects of external birefringence or the LD and LB of the sample on the observed signal, one predicts a slight reduction from the true value of the CD. However, the combined interaction of these two factors can cause serious measurement artifacts. Before we carry out the Jones matrix analysis, the pictorial representation given in Fig. 3 is instructive. From Subsection 2.D, the external birefringence of the optics before the sample converts the probe circularly polarized light beams into two perpendicular elliptically polarized beams. As in shown in Fig. 3, left (or right) elliptically polarized light can be viewed as possessing both circular and linear components. The two perpendicular linear components probe the LD of the sample and, along with the CD of the sample, contribute to the detected signal.

We now use the Jones matrix method to analyze this situation. However, it is important to note that M_{CD} and $M'_{LB,LD}$ do not commute. In Subsection 2.E we found that the N-matrix calculation results in a calculated signal that lies between the two limiting cases represented by the two noncommuting matrix products. For the combined effects of external birefringence and pump-induced linear dichroism (LD) and linear birefringence (LB), we will examine only the two limiting cases: (1) $M'_{LB,LD} \times M_{CD} \times M_{LB} \times J_{L,R}$ and (2) $M_{CD} \times M'_{LB,LD} \times M_{LB} \times J_{L,R}$. As before, in each of these two cases we will evaluate the effect of these additional polarization properties on the experimentally measured signal. A complete N-matrix treatment has been carried out; the results are given in Appendix A. The expression is significantly more complicated than those obtained for the two limiting cases. However, extensive numerical calculations show the contribution of these additional polarization properties as well as the isolation of the CD signal can be realized from the limiting-case calculations, which are given below.

For $M'_{LB,LD} \times M_{CD} \times M_{LB} \times J_{L,R}$, the calculated signal can be expressed as

$$\frac{E_L^2 - E_R^2}{E_L^2 + E_R^2} = \frac{k'^2 - k^2}{k^2 + k'^2} \cos 2b + \frac{m'^2 - m^2}{m^2 + m'^2} \times \frac{2kk'}{k'^2 + k^2} \sin 2\theta \sin 2b. \quad (48)$$

For $M_{CD} \times M'_{LB,LD} \times M_{LB} \times J_{L,R}$, the mathematical form of the calculated signal is more complicated. The order of matrix multiplication is now such that the contribution of pump-induced LB and LD to the experimental signal is overestimated. In this limit, we obtain

$$\frac{E_L^2 - E_R^2}{E_L^2 + E_R^2} = \frac{2mm'}{m^2 + m'^2} \frac{k'^2 - k^2}{k^2 + k'^2} \times (\cos 2\rho \cos 2b + \sin 2\rho \sin 2b \cos 2\theta) + \frac{m^2 - m'^2}{m^2 + m'^2} \sin 2\theta \sin 2b. \quad (49)$$

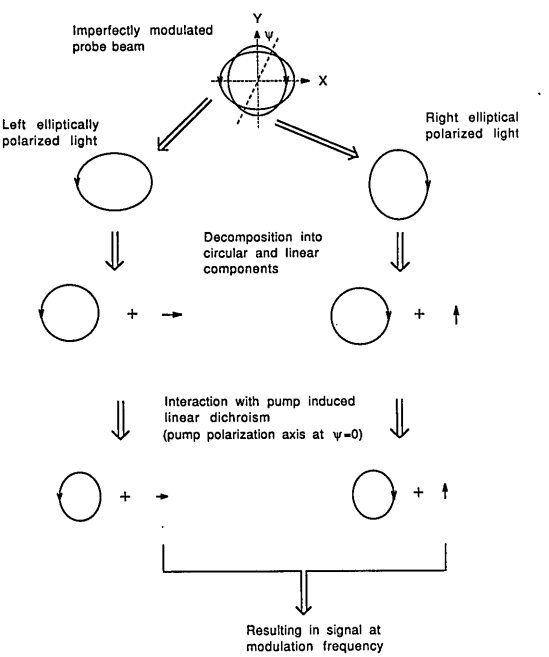

Fig. 3. Illustration of the effects of imperfectly modulated light and pump-induced linear dichroism. The left (or right) elliptically polarized light can be viewed as composed of a circular and a linear component. The two perpendicular linear components probe the linear dichroism induced by the pump beam and result in an additional signal at the modulation frequency.

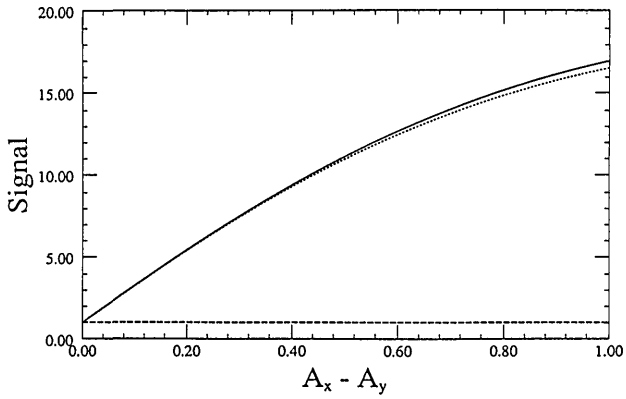

Fig. 4. The combined effect of the external birefringence of the optics and the pump-induced linear birefringence and linear dichroism of the sample on the measured signal is examined as a function of the magnitude of the pump-induced linear dichroism. Equations (48) (solid curve), (49) (dotted curve), and (18) (dashed line) are plotted. All curves are normalized to Eq. (18). The parameters used are $A_L = 5$, $A_R = 4.999$, $A_x = 5.0$, $b = 1°$, $\theta = 20°$, and $p = 5°$. These results show that a small amount of pump-induced LD can result in a large distortion of the data. The value of the true CD signal is given by the dashed line.

This expression represents the maximum effect that the various polarization properties of the experimental apparatus (optics and sample) can have on the determination of the transient CD value.

The first and second terms in Eqs. (48) and (49) are proportional to the CD and the LD of the sample, respectively. In general, the CD of the sample is small, $10^{-6} < \Delta\varepsilon/\varepsilon < 10^{-3}$; thus $2kk'/(k^2 + k'^2) \approx 1$, and the second terms in both expressions are identical. However, for most samples of interest the LD signal $(m^2 - m'^2)$ is generally 1 or 2 orders of magnitude larger than the CD signal $(k'^2 - k^2)$. Thus the second term in both expressions dominates the calculated signal, rendering the measurement of the CD essentially impossible. In addition to complicating the time-resolved CD measurement, this effect underlies the difficulty in measuring the CD of crystalline samples.[40] The effect of pump-induced LD on the signal can be seen from numerical calculations. In Fig. 4 we plot Eqs. (48) and (49), using the parameters $A_L = 5$, $A_R = 4.999$, $b = 1°$, $\theta = 20°$, and $\rho = 5°$. In calculating the x axis, we assumed that $A_x = 5$. For both expressions, a 20% difference between ε_x and ε_y results in more than an order-of-magnitude increase in signal over that expected from the pure CD of the sample.

4. EXPERIMENTAL RESULTS

In this section we examine experimental data on time-dependent signals observed in probing the N band of myoglobin (Mb) following photodissociation of CO from carbonmonoxy myoglobin (MbCO). For these experiments, the second harmonic of the cavity-dumped Nd:YAG laser was used for excitation (532 nm), and the third harmonic (355 nm) was used as the probe beam. This gives an ≈80-psec time resolution for the experimental apparatus. Pump and probe pulse energies were 60 and <1 μJ, respectively. Horse metMb was purchased from Sigma. The pH 7.0 phosphate buffer of MbCO was prepared as previously reported.[41] The Mb concentration was ≈0.9 mM with an optical density of ≈1.7 at 532 nm and ≈4.0 at 355 nm. Experimentally, the best signal-to-noise ratio is observed when one is using an optical density of ≈4 at the probe wavelength. A 50-mL sample was circulated through a 2-mm flow cell under CO atmosphere. Previous CD studies showed that MbCO has a negative CD signal at 355 nm of ≈−15. On the other hand, Mb is characterized by $\Delta\varepsilon = \varepsilon_L - \varepsilon_R \approx 0.0$.

A. Transient Signals Complicated by Pump-Induced Polarization Effects

First, we examine signals observed when using a linearly polarized pump pulse train. The optical arrangement is identical to that shown in Fig. 1, but the rotating half-wave plate in the pump beam has been removed. Under these conditions, the signals detected were close to unreproducible and exhibited a variety of behaviors. In Fig. 5, an example of the time-dependent signal is plotted. Following photolysis there is an increase in signal, followed by a long time tail, which shows a decrease in the CD signal. If one assumed that these data reflected the time-dependent CD signal, the two components of the decay in the CD signal could be attributed to different protein motions in the region of the heme ring. However, small changes in the alignment of the Pockels cell or the polarization of the pump beam has a large effect on the shape of the time-dependent curve. In addition to the behavior observed in Fig. 5, we have observed dip signals, in which the signal rises and then decays with a long tail. All these signals can be accounted for by considering the effect of pump-induced LD and LB on the experimental signal. As we mentioned in Subsection 2.E, using a polarized pump beam breaks the isotropy of the sample. As a result, the linear components of the elliptically polarized pump beam would probe the resulting LD of the sample; the magnitude of this signal would decay with a time constant that depends on the rotational motion of the protein.

In order to examine how the time-dependent pump-induced LD can affect the experimental results, we have carried out simulations of Eq. (48). Although this expression is a limiting case of the detected signal (the complex N-matrix calculation in Appendix A is required for deter-

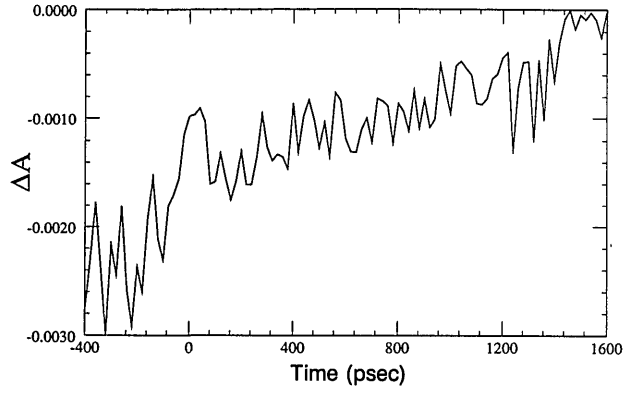

Fig. 5. An example of the experimental signal as a function of delay time is shown for the N band of Mb following photodissociation of CO from MbCO by using a linearly polarized pump beam. The signal shows a two-component change in the experimental signal. Comparison with theoretical calculations indicates that the data reflect dynamics caused by changes in both the CD of the sample and the pump-induced linear dichroism.

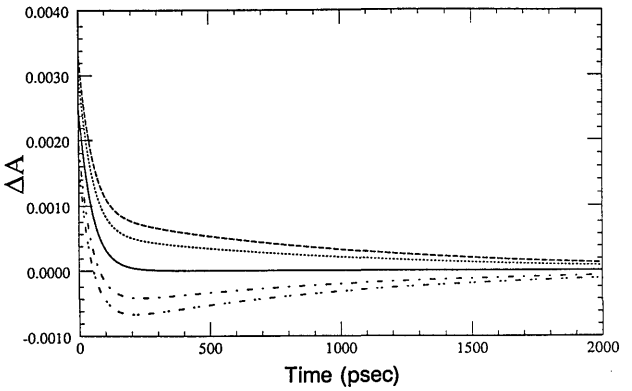

Fig. 6. Simulation of time-dependent signals using the time-dependent analog of Eq. (48). The linear and circular dichroism signals were assumed to relax exponentially with time constants of 1 nsec and 50 psec, respectively. The parameters used were $A_L = 5.0$, $A_R = 4.995$, $A_x = 5.0$, $A_y = 4.95$, $b = 1°$; $\theta = 0°$ (solid curve), $=20°$ (dotted curve), $=45°$ (dashed curve), $=-20°$ (single-dotted–dashed curve), $=-45°$ (double-dotted–dashed curve).

mination of the exact form of the experimental signal), the qualitative effects of the LD on the experimental CD signal can be gained from this expression. In Fig. 6 we show the calculated signals for five cases. In carrying out these simulations, we used values of 5.0, 4.995, 5.0, and 4.95 for the initial values of A_L, A_R, A_x, and A_y, respectively. These values correspond to a $\Delta A/A$ of 1×10^{-3} and 1×10^{-2} for the CD and the pump-induced LD, respectively, and are consistent with what one might expect for Mb. In the simulated case, the CD and LD signals were assumed to relax exponentially from their initial values to zero with time constants, τ_{CD} and τ_{LD}, of 50 psec and 1.0 nsec, respectively. The time dependence of the LD is expected to reflect both the overall rotation of the protein and the internal motion of the heme with respect to the surrounding protein matrix. On examination of the time-dependent form of Eq. (48), it is evident that the LD kinetics that occur on the time scale of CD change will contribute the most to distorting the true time dependence of the CD signal. For these reasons, a 1.0-nsec time constant is used to gauge the decay of the LD in carrying out the calculations shown in Fig. 6. A detailed study of the time-dependent LD data will be published shortly.[42] The external birefringence (b) was taken to be 1°, similar to that observed in the experimental apparatus. The signal was evaluated for five values of θ, the angle between the polarization axis of the pump beam and the axes defined by the linear components of the elliptically polarized probe beam. For the case of $\theta = 0$, the solid curve in Fig. 6, Eq. (48) reduces to expression (50):

$$\frac{E_L^2(t) - E_R^2(t)}{E_L^2(t) + E_R^2(t)} = \frac{k'^2(t) - k^2(t)}{k^2(t) + k'^2(t)} \cos 2b \approx \exp(-t/\tau_{CD}) \cos 2b. \quad (50)$$

Thus, in this case, the simulated signal reflects the true evolution of the time-dependent CD signal. Also plotted are the expected time-dependent signals for $\theta = +20°$, $+45°$, $-20°$, $-45°$. For positive angles, the effect of the LD term is to increase the signal observed at zero delay time, lengthen the time constant of the initial decay, and add a long decay-time tail to the signal. The magnitude of these effects increases with increasing values of θ. This behavior is similar to that associated with the experimentally observed data in Fig. 5. In addition, for values of $\theta < 0$ the effect of the LD is to cause an increase in the time constant of the initial decay, a change in sign of the CD signal, and a long decay component. This behavior has also been observed (data not shown). The calculations plotted in Fig. 6 demonstrate that even a small component of LD (1% in this calculation) can have a large effect on the time dependence of the signal. The mathematical expression given by Eq. (48) is not an accurate representation of the experimental signal. In this formula, the effects of pump-induced LB and LD are actually underestimated. Related simulations using Eq. (49) would overestimate the importance of these pump-induced polarization effects. Such calculations also generate curves quite similar to that plotted in Fig. 6. From our comparison of the N-matrix calculation with the limiting expression in Subsection 2.D, we know that the N-matrix calculation of the signal will give a result intermediate between those of Eqs. (48) and (49). This has been numerically verified by comparing the limiting cases with the N-matrix result given in Appendix A. Thus it is reasonable to assume that time-dependent simulations of the N matrix result would qualitatively give rise to curves whose time dependence is similar to that shown in Fig. 6. In either case, these results clearly show that, if one is to determine the true temporal evolution of the CD signal, the contributions from pump-induced LB and LD need to be removed.

B. Isolation of the Circular Dichroism Signal from Pump-Induced Polarizataion Effects

The method for removal of the effects of pump-induced LD and LB can be realized by considering their source. These contributions arise because the polarized photolysis beam preferentially excites molecules with transition dipole moments parallel to the polarization axis of the pump beam, thus breaking the isotropy of the sample. First, this problem can be eliminated by using a depolarized pump light. However, in practice, complete depolarization of a laser beam is difficult to achieve. Furthermore, in Subsection 4.A we demonstrated that even a small amount of LD, ≈1%, could lead to large changes in the observed data. We attempted to depolarize the pump beam, using a high-quality depolarizer; however, we were still unable to obtain a perfectly isotropic pump beam. Irreproducible results spanning the range of behavior shown in Fig. 6 were still observed. Second, if the polarization of the probe beam were perfectly circular, the pump-induced linear polarization effects would not be serious. However, owing to the strain birefringence of the optics, this is also not easily achieved: the probe beam consists of alternating orthogonally polarized ellipses (Subsection 2.D) and therefore probes the pump-induced LD of the sample.

A method for eliminating these effects can be seen by examining the functional form of the limiting cases of the detected signal, Eqs. (48) and (49). In both cases, the contribution of LD is contained in a term that is also a function of θ, the angle between the polarized vector of the

pump beam and the axes that define the LD in the sample. If this angle were a linear function of time, $\theta(t)$, then the LD would be modulated at the rotation frequency of 2θ. If this modulation frequency were significantly different from the modulation frequency that contains the CD signal, phase-sensitive detection could discriminate between the CD of the sample and the pump-induced LB and LD. Experimentally, this is achieved by spinning a half-wave plate in the pump beam at a frequency of 3.5 Hz. This generates the necessary rotation of the polarization vector of the pump beam and consequently a modulation of the LD signal. With a time constant (3–10 sec) much longer than the rotation cycle of the half-wave plate, this modulated signal can easily be distinguished and suppressed by the lock-in amplifier.

In this case, the observed signal no longer contains contributions from the pump-induced LD, and terms in Eqs. (48) and (49) that depend on θ are not detected at the 500-Hz modulation frequency. The reduced expressions would still represent limiting equations for the detected signal; the experimental signal will be intermediate between these expressions. Averaging Eqs. (48) and (49) over θ results in the following limits for the detected signal:

$$\frac{k'^2 - k^2}{k^2 + k'^2}\cos 2b \geq \frac{E_L^2 - E_R^2}{E_L^2 + E_R^2} \geq \frac{k'^2 - k^2}{k^2 + k'^2}\frac{2mm'}{m^2 + m'^2}\cos 2\rho \cos 2b. \quad (51)$$

The first term in relation (51) is identical to the signal obtained in steady-state CD measurements. Only the strain birefringence of the optics diminished the observed signal from the true value of the CD of the sample. At the other extreme, the measurement is reduced by three factors, the strain birefringence ($\cos 2b$), the pump-induced birefringence ($\cos 2\rho$), and a term that is dependent on the transmission of the linear components on the probe beam. In practice, when a depolarizer (or quarter-wave plate) is used in the pump beam, the two addition factors in this limit, $2mm'/(m^2 + m'^2)$ and $\cos 2\rho$, are both nearly 1. As an example, for the case calculated in Fig. 6, where $A_x = 5$ and $A_y = 4.95$, the term $2mm'/(m^2 + m'^2)$ results in a correction factor of 0.998. This effect is negligible. In carrying out time-dependent studies, a noncollinear geometry between the pump and probe beams is used. As a result, the projection of the polarization axis of the pump beam on the coordinate system defined by the probe is a function of θ. This affects the modulation of the pump-induced LD. In Appendix B it is shown that for small angles between the pump and probe beams this effect is also negligible.

It is also worth pointing out that the same technique can be applied to steady-state CD measurements of crystalline samples. As we discussed in Subsection 2.E, the mathematics of pump-induced LB and LD effects are identical to those used to describe anisotropic uniaxial crystals. Thus techniques similar to those described above could be used to collect accurate steady-state CD spectra of such materials. In practice, one could rotate the sample or use a rotating half-wave plate in the modulated probe beam to eliminate the LB and LD signals.

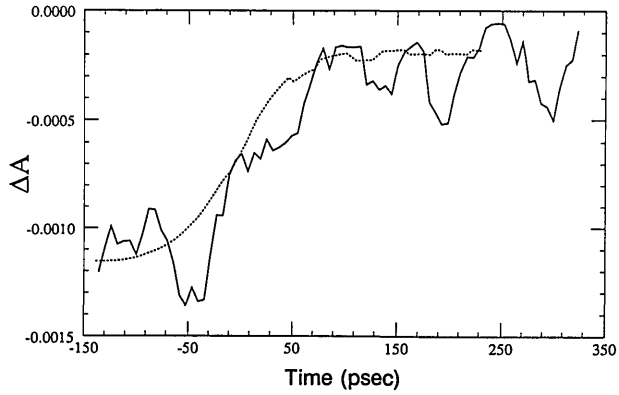

Fig. 7. The CD value at 355 nm is plotted as a function of time following excitation of MbCO by 532-nm light. The polarization of the photolysis light was modulated with a spinning half-wave plate, removing contributions of pump-induced LD and LB to the signal detected at the 500-Hz modulation frequency. Within the signal-to-noise ratio shown, the data suggest that the confirmational relaxation in Mb following ligand dissociation occurs within 100 psec of photolysis. The dashed curve is a measure of the transient absorption dynamics, indicating the instrument response function.

In Fig. 7, time-dependent CD data for the N band of Mb following the photoelimination of CO from MbCO by using the rotating half-wave plate in the pump beam are shown. These results are free from the pump-induced linear polarization effects and reveal the evolution of the CD signal of the protein in time. These data are to our knowledge the first direct picosecond measurement of the protein CD following photodissociation and reveal information concerning the time scale of the relaxation of the protein structure following ligand dissociation. The signal evolves from that characteristic of MbCO ($\Delta\varepsilon \approx 15$) to that expected for Mb ($\Delta\varepsilon \approx 0$) of the order of the instrument response, 100 psec, which indicates that the protein structure in the vicinity of the heme ring relaxes on a time scale of tens of picoseconds. The value of the CD observed for delay times larger than 100 psec ($\Delta\varepsilon \approx -1$) is not exactly equal to that of Mb ($\Delta\varepsilon \approx 0$). This is most likely because our excitation beam photolyzes ≈90% of the MbCO in the region interrogated by the probe beam. However, as we explain in Appendix B, one might also need to consider the effects of the noncollinear geometry of the pump and probe beams. We are currently examining new approaches for improving the signal-to-noise ratio of the experiment as well as carrying out studies on the Soret band of Mb. Using a piezoelectric modulator to generate the circularly polarized probe pulses has increased the signal-to-noise ratio of the experiment by a factor of ≈10. This has resulted in the ability to resolve the relaxation of the CD signal in the photodissociation of MbCO. A protein relaxation time of ≈80 psec is revealed. A detailed account of the work can be found elsewhere.[42–44]

CONCLUSIONS

We have analyzed an experimental approach for collecting time-resolved CD data on proteins. Jones matrix calculus was used to examine the effects of various polarization properties of both the apparatus and the sample on the observed signal.

There are two significant advances afforded by the approach discussed in this paper. First, the use of polarization modulation instead of a time-dependent ellipticity apparatus eliminates several severe polarization effects, which can complicate the experimental signal. Significant advantages of polarization-modulation techniques over ellipticity in carrying out static CD measurements have been discussed in several review papers. We have shown that many of these same advantages carry over into the time-resolved regime. Second, the time resolution is limited by the laser pulse width, not by the polarization-modulation frequency, as is commonly believed. With recent advances in the ultrafast laser field, subpicosecond time resolution can be achieved.

The technique was applied to examine the time-dependent CD signal of the N band of Mb following the photodissociation of CO from MbCO. These data suggest that, following photodissociation, the protein undergoes conformation relaxation within 100 psec.

APPENDIX A

In this appendix the form of the experimental signal is rigorously derived, using the N-matrix formalism. In this case, the intensities of the transmitted light beams, E_L^2 and E_R^2, can be derived from the product of the matrices $M_{LB,LD,CD} \times M_{LB} \times J_L$ and $M_{LB,LD,CD} \times M_{LB} \times J_R$, respectively. The functions of forms of $M_{LB,LD,CD}$ and M_{LB} are given by Eqs. (45) and (26), respectively. The evaluation is tedious but straightforward and results in the following calculated signal:

$$\frac{E_L^2 - E_R^2}{E_L^2 - E_R^2} = \frac{\gamma[Q\cosh(Qz)\sinh(\bar{Q}z) + \bar{Q}\sinh(Qz)\cosh(\bar{Q}z)}{Q\bar{Q}\cosh(Qz)\cosh(\bar{Q}z) + (g^2 + \beta^2 + \gamma^2)\sinh(Qz)\sinh(\bar{Q}z)} f(\theta, b)$$
$$- \frac{\bar{Q}(\beta - ig)\sinh(Qz)\cosh(\bar{Q}z) + Q(\beta + ig)\sinh(\bar{Q}z)\cosh(Qz)}{Q\bar{Q}\cosh(Qz)\cosh(\bar{Q}z) \times (g^2 + \beta^2 + \gamma^2)\sinh(Qz)\sinh(\bar{Q}z)} g(\theta, b)$$
$$- \frac{2\gamma g \sinh(\bar{Q}z)\sinh(Qz)}{Q\bar{Q}\cosh(Qz)\cosh(\bar{Q}z) + (g^2 + \beta^2 + \gamma^2)\sinh(Qz)\sinh(\bar{Q}z)} h(\theta, b), \quad \text{(A1)}$$

where

$$f(\theta, b) = \tfrac{1}{2}[\cos 2b(\cos 4\theta + 1) - \cos 4\theta + 1], \quad \text{(A2)}$$

$$g(\theta, b) = \sin 2\theta \sin 2b, \quad \text{(A3)}$$

and

$$h(\theta, b) = \cos 2\theta \sin 2b. \quad \text{(A4)}$$

The first term in Eq. (A1) is the product of $f(\theta, b)$ and the result obtained in Subsection 2.E, Eq. (46). Numerical simulations of this expression show that the values obtained are intermediate between those calculated with the limiting expression, Eqs. (48) and (49). Equations (A1)—(A4) are, however, the exact representation of the observed signal and accurately account for the effects of pump-induced birefringence and dichroism and the coupling of these effects to the strain birefringence of the optical elements. The effect of the rotating-wave plate in the pump beam can be seen by averaging θ in the above expressions over the cycle from 0 to 2π. In this case, we find that both the second and the third terms in Eq. (A1) do not contribute to the signal; the total signal arises from the first term. This expression satisfies the inequality given in relation (51), confirming that the pump-induced polarization effects are eliminated.

APPENDIX B

In our experimental apparatus, a noncollinear arrangement is used for the pump and probe laser beams. A collinear pump–probe geometry would require optics in the probe beam following the modulator. These optics could affect the polarization of the modulated probe beam. However, with a small angle between the pump and the probe beams, a short-path-length sample cell, matched beam waists at the sample, and carefully chosen sample concentration and pump and probe wavelengths, the pump beam can excite a large percentage (>90%) of the molecules in the region interrogated by the probe beam.

As we discussed above, a rotating half-wave plane in the pump beam is used to randomize the polarization of the beam during the course of a measurement (3–10-sec time constant). On the average, this results in an isotropic excitation. However, in a noncollinear pump–probe geometry the probe beam experiences an excitation anisotropy. Should the probe beam be imperfectly modulated or distorted by the birefringence of the optics, this pump-induced LD would interfere with the CD measurement. In this appendix, we determine the magnitude of this effect for our experimental setup.

The maximum interference happens when the two orthogonal ellipses of the modulated probe beam have their long axes along the x and y axes ($\theta = 45°$). The left and right elliptically polarized light beams can each be decomposed into two linear polarization components along the x and y directions; each experiences different absorption owing to the pump-induced LD of the sample. In this case, the transmitted beams I_L and I_R are

$$I_L = I_{Lx} + I_{Ly} = (I_{Lx})_0 10^{-A_x} + (I_{Ly})_0 10^{-A_y} \quad \text{(B1)}$$

and

$$I_R = I_{Rx} + I_{Ry} = (I_{Rx})_0 10^{-A_x} + (I_{Ry})_0 10^{-A_y}, \quad \text{(B2)}$$

where I_{Lx}, I_{Ly}, I_{Rx}, and I_{Ry} are the x and y components of the left and right elliptically polarized probe beams, respectively.

According to expression (15), the measured CD signal is

$$\Delta A = \frac{\Delta I}{2.303 \times I} = \frac{I_L - I_R}{2.303 \times (I_L + I_R)/2}. \quad \text{(B3)}$$

Under our experimental condition, the worst modulation of the probe laser light generated two elliptical

polarized beams with a ratio of the short to long axes of 9:10, giving

$$\frac{(I_{Lx})_0}{(I_{Ly})_0} = \frac{9}{10}, \qquad \frac{(I_{Rx})_0}{(I_{Ry})_0} = \frac{10}{9}. \tag{B4}$$

Substituting Eqs. (B1), (B2), and (B4) into Eq. (B3), and noting that $|A_x - A_y|$ is small, one obtains the following expression:

$$\Delta A = \frac{|10^{-A_x} - 10^{-A_y}|}{2.303 \times 19 \times (10^{-A_x} + 10^{-A_y})/2} \approx \frac{|A_x - A_y|}{19}. \tag{B5}$$

From Eq. (B5), the magnitude of the excitation anisotropy can be determined. In a typical LD experiment in which linearly polarized light is employed as the pump beam, the induced absorption anisotropy, $|A_x - A_y|/A$, is of the order of 10^{-1}. In our experiment, an isotropic pump beam is focused on the sample at an angle of $\eta = 7°$ with respect to the probe. This results in a projection of $\cos \eta = 0.9925$ on the horizontal axes, as defined by the probe beam. This reduces the excitation anisotropy by a factor of 0.0075. As a result, with a sample optical density of 4 at the probe wavelength, the maximum signal that arises from the pump-induced LD as a result of the noncollinear pump–probe geometry is $\Delta A = 1.6 \times 10^{-4}$. In the case of Mb, this value of ΔA corresponds to $\Delta\varepsilon \approx 1$. This value is negligible compared with the changes observed in the N or Soret bands following photodissociation.

ACKNOWLEDGMENTS

This research is supported by the Presidential Young Investigator Program of the National Science Foundation. We thank David Kliger for many helpful discussions and Cora Einterz for suggestions on the modeling of the combined effects of linear birefringence, linear dichroism, and circular dichroism.

J. D. Simon is a National Science Foundation Presidential Young Investigator 1985–1990, an Alfred P. Sloan Fellow 1988–1990, and a Camille and Henry Dreyfus Teacher–Scholar, 1990–1995.

REFERENCES

1. A. F. Drake, J. Phys. E **30,** 170 (1986).
2. H. P. Jensen, J. A. Schellman, and T. Troxell, Appl. Spectrosc. **32,** 192 (1978).
3. J. A. Schellman, in *Polarization Spectroscopy of Ordered Systems,* B. Samori and E. W. Thulstrup, eds. (Kluwer, Hingham, Mass., 1988).
4. J. Michl and E. Thulstrup, *Spectroscopy with Polarized Light* (VCH, New York, 1986).
5. J. Schellman and H. P. Jensen, Chem. Rev. **87,** 1359 (1987).
6. G. R. Fleming, *Chemical Applications of Ultrafast Spectroscopy* (Oxford U. Press, Oxford, 1986).
7. D. Waldeck, A. J. Cross, D. B. McDonald, and G. R. Fleming, J. Chem. Phys. **74,** 3381 (1981).
8. D. H. Waldeck and G. R. Fleming, J. Phys. Chem. **85,** 2614 (1981).
9. A. J. Cross, D. H. Waldeck, and G. R. Fleming, J. Chem. Phys. **78,** 6455 (1983).
10. A. von Jena and H. E. Lessing, Appl. Phys. **19,** 131 (1979).
11. A. von Jena and H. E. Lessing, Ber. Bunsenges. Phys. Chem. **83,** 181 (1979).
12. C. V. Shank and E. P. Ippen, Appl. Phys. Lett. **26,** 62 (1975).
13. D. Reiser and A. Laubereau, Chem. Phys. Lett. **92,** 297 (1982).
14. G. S. Beddard and M. J. Westby, Chem. Phys. **57,** 121 (1981).
15. G. L. Easley, M. D. Levenson, and W. M. Tolles, IEEE J. Quantum Electron. **QE-14,** 45 (1978).
16. A. Owyoung, IEEE J. Quantum Electron. **QE-14,** 192 (1978).
17. See for example C. R. Cantor and P. R. Schimmel, *Biophysical Chemistry* (Freeman, New York, 1980).
18. Y. Sugita, M. Nagai, and Y. Yoneyama, J. Biol. Chem. **246,** 383 (1971).
19. R. Woody, in *Biochemical and Clinical Aspects of Hemoglobin Abnormalities,* W. S. Caughey, ed. (Adademic, New York, 1978).
20. M-C. Hsu and R. Woody, J. Am. Chem. Soc., **91,** 3679 (1969).
21. M-C. Hsu and R. Woody, J. Am. Chem. Soc. **93,** 3515 (1971).
22. S. Beyshok, I. Tyuma, R. E. Benesch, and R. Benesch, J. Biol. Chem. **242,** 2460 (1967).
23. S. R. Simon and C. R. Cantor, Proc. Natl. Acad. Sci. (USA) **63,** 205 (1969).
24. P. M. Bayley and M. Anson, Biopolymers **13,** 401 (1974).
25. F. A. Ferrone, J. J. Hopfield, and S. E. Schnatterly, Rev. Sci. Instrum. **45,** 1392 (1974).
26. D. S. Kliger and J. W. Lewis, Rev. Chem. Intermed. **8,** 367 (1987).
27. J. W. Lewis, R. F. Tilton, C. M. Einterz, S. J. Milder, J. D. Kumtz, and D. S. Kliger, J. Phys. Chem., **89,** 289 (1985).
28. C. M. Einterz, J. W. Lewis, S. J. Milder, and D. S. Kliger, J. Phys. Chem. **89,** 3845 (1985).
29. S. J. Milder, S. C. Bjorling, I. D. Kuntz, and D. S. Kliger, *Biophys. J.* **53,** 659 (1988).
30. X. Xie and J. D. Simon, Rev. Sci. Instrum. **60,** 2614 (1989).
31. R. C. Jones, J. Opt. Soc. Am. **31,** 488 (1941).
32. R. C. Jones, J. Opt. Soc. Am. **31,** 493 (1941).
33. R. C. Jones, J. Opt. Soc. Am. **31,** 500 (1941).
34. R. C. Jones, J. Opt. Soc. Am. **32,** 486 (1942).
35. R. C. Jones, J. Opt. Soc. Am. **37,** 107 (1947).
36. R. C. Jones, J. Opt. Soc. Am. **37,** 110 (1947).
37. R. C. Jones, J. Opt. Soc. Am. **38,** 671 (1948).
38. X. Xie and J. D. Simon, Opt. Commun. **69,** 303 (1989).
39. D. S. Kliger, J. W. Lewis, and C. E. Randall, *Polarized Light in Optics and Spectroscopy* (Academic, Orlando, Fla., 1990).
40. S. B. Piepho and P. N. Schatz, *Group Theory in Spectroscopy, with Applications to Magnetic Circular Dichroism* (Wiley, New York, 1983).
41. T. Samejima and J. T. Yang, J. Mol. Biol. **8,** 863 (1964).
42. X. Xie and J. D. Simon, "Time-resolved dichroism and absorption studies of protein relaxation following photo-chemical elimination of CO from carbonmonoxy myoglobin," submitted to Biochemistry.
43. X. Xie and J. D. Simon, "Picosecond time-resolved circular dichroism study of protein relaxation in myoglobin," submitted to J. Am. Chem. Soc.
44. X. Xie and J. D. Simon, "Picosecond circular dichroism spectroscopy: experiment, theory, and applications to protein dynamics," in *Time-Resolved Laser Spectroscopy in Biochemistry II,* J. Lakowitz, ed. Proc. Soc. Photo-Opt. Instrum. Eng. **1204,** 66 (1990).